Electrochemical and Solid-State Letters, **8** (3) A141-A144 (2005)
1099-0062/2005/8(3)/A141/4/$7.00 © The Electrochemical Society, Inc.

Unexpected 5 V Behavior of Zn-Doped Mn Spinel Cathode Material

Y. Ein-Eli,[a,*,z] W. Wen,[b,] and S. Mukerjee[b,*]**

[a]*Department of Materials Engineering, Technion-Israel Institute of Technology, Haifa 32000, Israel*
[b]*Department of Chemistry and Chemical Biology, Northeastern University, Boston, Massachusetts 02115, USA*

Zn-doped Mn spinel was investigated for its unique 5 V reversible Li intercalation. Only at a certain Zn doping, $LiZn_{0.25}Mn_{1.75}O_4$, lithium ions can be extracted at 5 V, while at high Zn doping of $LiZn_{0.5}Mn_{1.5}O_4$ no reversible capacity was observed. Electrochemical extraction of lithium ions during charge at 5 V is partially reversible. The two Zn doped compositions ($x = 0.25$ and 0.5 in $LiZn_xMn_{2-x}O_4$) have a single phase cubic spinel structure, possessing a primitive cubic atomic arrangement, in contrast to the face centered cubic $LiMn_2O_4$ spinel. All materials synthesized have a tetradecahedra grain structure, bonded via the hexagon facets.
 [DOI: 10.1149/1.1857672]

Manuscript submitted August 12, 2004; revised manuscript received September 26, 2004. Available electronically January 19, 2005.

$LiMn_2O_4$ is still regarded as a prospective cathode material for the next generation of lithium batteries. It has a face-centered cubic (FCC) spinel structure with lithium and Mn ions occupying the tetrahedral sites and octahedral sites, respectively. The theoretical specific capacity of this material is 148.2 mAh/g, with the characteristic two-step charge-discharge behavior which is attributed to the existence of two cubic structures[1] in the charging and discharging process. However, this material suffers from a cubic to tetragonal distortion[2] at or near its discharged state due to imbalance of the Mn^{3+}/Mn^{4+} ratio leading to higher presence of Jahn-Teller active Mn^{3+}. Such structural changes lead to domain fractures and consequent lowering of cycle life. However, doping the Mn spinel with other low valence state transition metal ions can increase the overall Mn oxidation state and minimize Jahn-Teller distortion.[3,4]

One highly interesting phenomenon associated with such doping of low valence state transition elements is the corresponding RedOx behavior observed at elevated potentials (close to 5 V) as compared to the $Mn^{3+}/Mn^{4+} \rightarrow Mn^{4+}$ which typically shows two plateaus between 4-4.5 V. These higher potential plateaus are observed both at room and elevated temperatures.[5] Much work has being focused on the elevated potential behavior ($\sim$5 V) of this material during the last decade.[3-17] Typical examples of such dopants are Cu,[3,4,6,7] Co,[7,8] Cr,[7,8,10,11] Fe,[6,7] and Ni.[7-9,16] It is normally believed that the charge compensation as a result of the doping process increases the Mn^{4+} ratio, compensating lithium extraction at the elevated potential plateau during the anodic charge process, as have been observed with Ni[9,12] and Cu[3,4] doped systems.

In addition to the doped samples, $LiMn_2O_4$ thin film deposited[13] by electron beam evaporation or radio-frequency (rf) sputtering and nonstoichiometric $Li_{1+x}Mn_2O_{4+\delta}$ samples[14] also exhibit such elevated potential plateaus. The general consensus is that such elevated potential plateaus are due to the extraction of lithium ions from octahedral sites. According to Thackeray,[15] the existence of two intergrown spinel compounds, such as $Li_{8a}[Mn_2]_{16d}O_4$ and $Li_{8b}[Mn_2]_{16c}O_4$ in $LiMn_2O_4$ thin films, where 8*a* and 8*b* refer to tetrahedral sites and 16*d* and 16*c* refer to octahedral sites, are responsible for the observance of such a separate intercalation potentials (different sites possessing separate chemical potentials).

In the context of doping with low valence transition elements, many researchers have explored Zn substituted Mn spinel materials as possible cathode materials in Li-ion battery technology.[7,18] However, all the prior studies concluded that for the composition of $LiZn_{0.5}Mn_{1.5}O_4$ no contribution from Zn to overall electrochemical activity was possible.[18] Prior report on Zinc ($LiZn_{0.5}Mn_{1.5}O_4$) substituted spinel material has shown Li occupancy in octahedral sites using ^{7}Li solid state nuclear magnetic resonance (NMR).[18] This suggests that Zn ions occupy tetrahedral positions, forcing some fraction of lithium ions into octahedral sites. However, these studies report on a single material composition, such as $LiZn_{0.5}Mn_{1.5}O_4$, cycled up to 5 V, while other compositions of $LiZn_xMn_{2-x}O_4$ remain unexamined both in terms of composition and potential window of charge/discharge.

In this short communication we report, for the first time, 5 V activity of Zn-doped Mn spinel material. The observed behavior is investigated with Zn substitution in the range $LiZn_xMn_{2-x}O_4$, where x in the range $0 \leqslant x \leqslant 0.5$. Zn being at the end of the first row transition series is an important dopant element because it allows for better modeling of the behavior at elevated potentials. The filled d-shells of Zn enforce that as a consequence of charge compensation all Mn associated with Zn would be in the +4 valence state.

Experimental

Samples with the general composition of $LiZn_xMn_{2-x}O_4$ with $x = 0$, 0.25, and 0.5, were prepared from the acetate salts (Li acetate, Mn acetate, and Zn acetate, Fluka) using low temperature sol-gel techniques described in detail elsewhere.[3,4] X-ray diffraction (XRD) patterns of the synthesized powdered materials were recorded using a Philips X'pert Diffractometer (PW3040/60). Evaluation and examination of grain size and images was conducted with the use of high-resolution scanning electron microscope (Hitachi S-4800).

Electrodes were cast (doctor bladed) using a slurry comprising of 80% spinel Mn oxide, 10% carbon black (Shawinigan Acetylene black), and 10% polyvinylidene binder with a fugitive solvent (1 methyl-2 pyrrolidinone) on an aluminum substrate ($\sim$5 μm), dried at 120°C under vacuum for 2 h.

Electrochemical tests were performed in a PTFE T cell containing Li foil anode and Li reference electrode. Details of the electrochemical tests are given in reference.[3,4] Cells were tested in the voltage plateau of 3.3-5.4 V. Electrolyte used in this investigation composed of ethylene carbonate and dimethyl carbonate mixture in a volume ratio of 1:1 containing 1 M $LiPF_6$ salt (EM Industries).

Results and Discussion

Materials characterization XRD measurements.—Figure 1 presents XRD patterns of three Zn-doped materials with Zn composition of $x = 0.0$, 0.25, and 0.5 in $LiZn_xMn_{2-x}O_4$, (Fig. 1a-c, respectively). Nearly phase-pure Zn doped materials exhibited XRD patterns which were somewhat different from the diffraction pattern obtained from $LiMn_2O_4$, wherein a significantly higher number of diffraction peaks are observed in the former. The existence of a contaminant phase, with insignificant concentration, most probably

* Electrochemical Society Active Member.
** Electrochemical Society Student Member.
z E-mail: eineli@tx.technion.ac.il

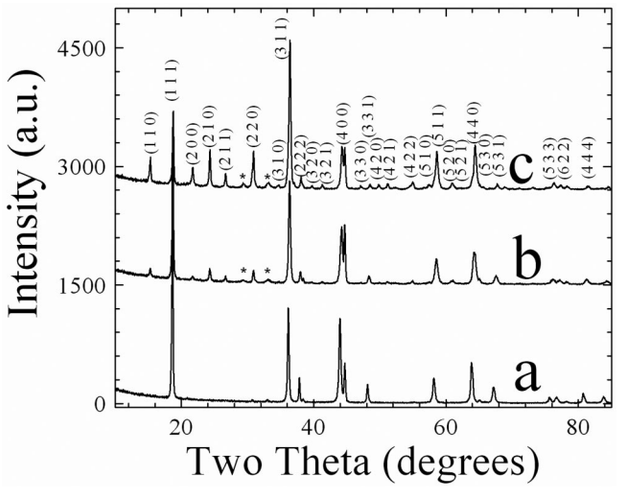

Figure 1. XRD pattern (Cu Kα) for $LiZn_xMn_{2-x}O_4$ powders, where x = (a) 0, (b) 0.25, and (c) 0.5.

due to the formation of $ZnMn_2O_4$ spinel (peaks positioned at 2 theta of 29.3° and 33.1°, marked in Fig 1b and c) is observed in the Zn doped powder materials. The intensity of some diffraction peaks which are not observed in the pristine $LiMn_2O_4$ XRD pattern, such as 110, 200, and 210, increases as the Zn content increases. This suggests that Zn ions may be occupying tetrahedral sites in the crystal lattice. $LiZn_{0.5}Mn_{1.5}O_4$ was indexed as a cubic structure with a lattice parameter of 8.17 Å, using powder indexing module in the Cerius[2] program. Furthermore, the Zn doped spinels with Zn content of 0.25 and 0.5 have similar XRD diffraction patterns, which suggest that their crystal structures are similar. The patterns for Zn-doped spinel materials were indexed to provide for a primitive cubic structure compared with face centered cubic $LiMn_2O_4$ spinel structure. Moreover, the existence of the 200 and 400 planes, and the absence of the 100 plane in the spectra may suggest the existence of a 2_1 screw axis at the 100 plane. Thus, the Zn substituted Mn spinel compounds belong to a P 2_1 3 space group. Hence, referring to the compositions of $LiZn_xMn_{2-x}O_4$ (with x = 0.25 and 0.5) as Zn doped Mn-spinels is incorrect and we henceforth refer to them as cubic Zn-modified $LiMn_2O_4$.

High-resolution scanning electron microscopy (HRSEM).—Figure 2 presents HRSEM images obtained from three samples of composition; $LiZn_xMn_{2-x}O_4$ with x = 0.0, 0.25, and 0.5 (Fig. 2a, c, and e, respectively). All three materials have a truncated octahedral structure (tetradecahedra), having six squares and eight hexagons, with side lengths of 60-100 nm. Although there are two ways for co-joining two tetradecahedra units and 6 possibilities for three tetradecahedra blocks to be linked, the SEM micrographs (Fig. 2b, d, and f) reveal that the truncated octahedrals are bonded via the hexagon facets. Observance of such well defined faceted structures is reported here for the first time to the best of our knowledge. These ''single crystal'' like structures are important in understanding intradomain interactions and grain fracture as a result of cycling.

Electrochemical characterization. Slow scan cyclic voltammetry (SSCV).—Figure 3 shows SSCV of three samples with and without Zn-doping with Zn composition of x = 0.0, 0.25, and 0.5 in $LiZn_xMn_{2-x}O_4$ (Fig. 3a-c, respectively). The two-step charge and discharge profile at 4 V region for x = 0.25 in $LiZn_xMn_{2-x}O_4$ is well resolved as evident from Fig. 3b, albeit with a lower resolution as compared to the corresponding behavior for $LiMn_2O_4$ (Fig. 3a). The 5 V behavior is clearly observed for the $LiZn_xMn_{2-x}O_4$ composition containing x = 0.25. However, no electrochemical activity is observed for the x = 0.5 in composition ($LiZn_xMn_{2-x}O_4$),

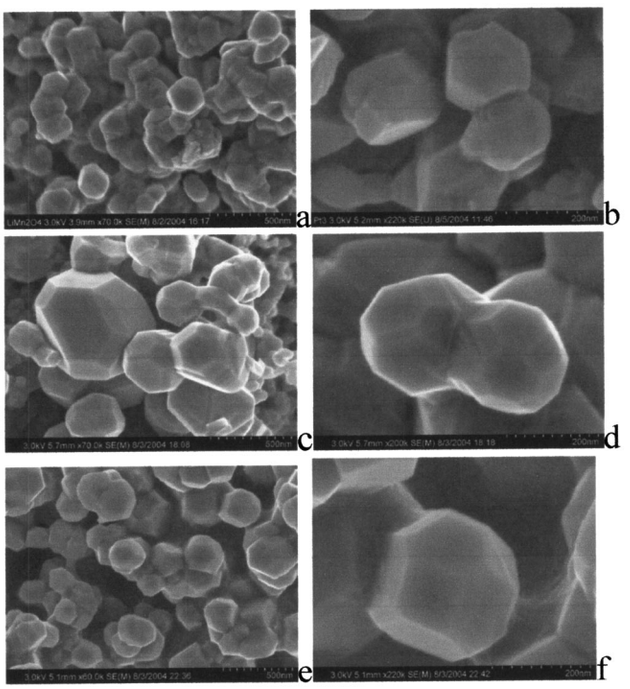

Figure 2. HRSEMs obtained from three Zn-doped materials with Zn composition of (a and b) x = 0.0; (c and d) x = 0.25 and (e and f) x = 0.5 in $LiZn_xMn_{2-x}O_4$.

both in the 4 and 5 V regions, in agreement with earlier report.[18] Furthermore, the 5 V behavior observed for the composition $LiZn_{0.25}Mn_{1.75}O_4$ is not completely reversible, as the 5 V peak observed during the back-scan (cathodic process) is much smaller than the corresponding anodic peak. Surprisingly, a small 5 V reversible behavior is also found upon scanning the undoped $LiMn_2O_4$ material, as can be seen in the inset of Fig. 3a. This may suggest that Zn doping is not the origin of the 5 V behavior. However, the significant

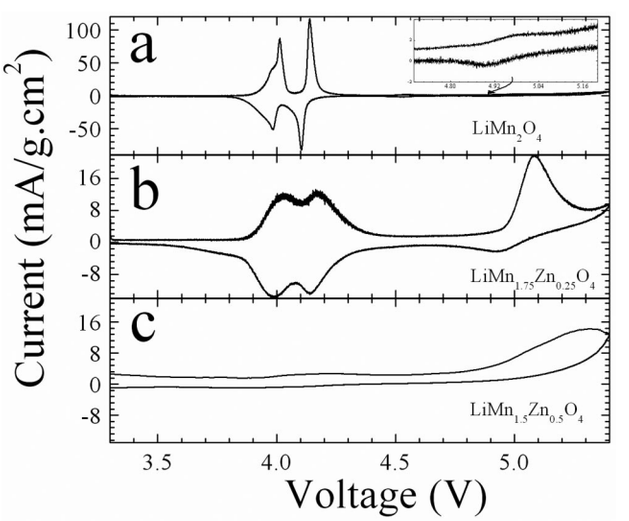

Figure 3. SSCV (20 μV/s) of three Zn-doped materials with Zn composition of x = (a) 0.0, (b) 0.25, and (c) 0.5 in $LiZn_xMn_{2-x}O_4$. Li metal served as anode and reference electrodes.

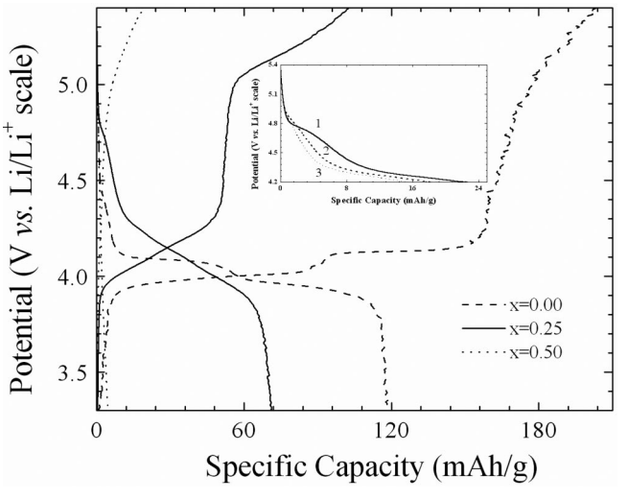

Figure 4. Chronopotentiograms (0.1 mA/cm^2) of three Zn-doped materials with Zn composition of (dashed line) $x = 0.0$; (solid line) $x = 0.25$ and (dotted line) $x = 0.5$ in $LiZn_xMn_{2-x}O_4$. Upper potential window of 4.2 and 5.4 V is shown in the inset presenting the first three consecutive discharge cycles obtained from cycling $LiZn_{0.25}Mn_{1.75}O_4$. Li metal was served as an anode.

anodic peak in the SSCVs obtained from the Zn doped material indicates that Zn doping is necessary to facilitate the 5 V behavior.

Chronopotentiometric studies.—Three totally different types of electrochemical behavior are observed for the three $LiZn_xMn_{2-x}O_4$ materials compositions, where $x = 0.0$, 0.25, and 0.5, as evident from Fig. 4. The Zn-doped material with Zn content of 0.25 exhibits two potential plateaus, which are located at 4 and 5 V, separated by a potential jump between 4.3 and 5 V. These two regions can also be seen in the discharge step, although the discharge capacity at 5 V is much smaller (25 mAh/g) as compared to the corresponding charge capacity (50 mAh/g), pointing to a poor reversibility and a possible electrolyte oxidation at 5 V. Nevertheless, the 5 V electrochemical activity is still observed (although reduced discharge capacity is being recorded at each cycle) at the following consecutive 3 cycles, as shown in the inset in Fig. 4. It is also observed that the specific discharge capacity at 4 V region increases with decrease in the Zn content in the ceramic compounds (almost no capacity at $x = 0.5$ to 50 mAh/g at $x = 0.25$ and 120 mAh/g at $x = 0$ in $LiZn_xMn_{2-x}O_4$), which can be correlated to a decrease in the content of Mn^{3+} ions in the crystal lattice. This is manifest in the extremely small capacity, of less than 5 mAh/g, for $LiMn_{1.5}Zn_{0.5}O_4$ material, having a nominal Mn oxidation state of +4. Furthermore, the 5 V behavior is completely absent. Thus, it is believed that the oxidation of Mn ions from a +4 state to a higher oxidation state is not the origin for the 5 V behavior observed with the specific composition of $LiZn_{0.25}Mn_{1.75}O_4$. The characteristic well-known two-step charge and discharge profiles, around 4 V region, typical for $LiMn_2O_4$, are also seen for the Zn-doped material with a composition of 0.25, albeit with a much smaller resolution. The existence of two step behavior with a lower resolution as compared to those typically observed for nondoped Mn spinel suggests a different intercalation environment due to Zn doping. This is supported by our XRD data where Zn doping causes a transition to a primitive cubic structure from a FCC spinel. Taking into a consideration that all zinc ions reside in 8*a* lithium tetrahedral sites, while some Li cations reside also in the octahedral 16*d* site, yielding a material formulated as $[Li_{0.75}Zn_{0.25}]_{8a}[Mn_{1.25}{}^{(+4)}Mn_{0.5}{}^{(+3)}Li_{0.25}]_{16d}O_4$, it is expected that at the 4 V region the overall theoretical capacity would be ~70 mAh/g, while the theoretical capacity at the 5 V, related to the extraction of Li from octahedral sites would be ~35 mAh/g. The experimental discharge capacities obtained both at the 4 V (50 mAh/g) and at the 5 V (25 mAh/g) regions are in good agreement with the theoretical calculations.

Zinc, cadmium, and mercury belong to Group IIB (12) elements, having two *s* electrons outside filled *d* shells. These elements follow Cu, Ag and Au in their electronic structures. Whereas in Cu, Ag, and Au, the filled *d* shells fairly readily lose one or two *d* electrons to yield ions or complexes in the II and III oxidation states, this was never reported or anticipated from Group IIB (12) elements.[19] The high potential activity of the low doped Zn spinel material cannot be attributed to an alteration in Zn ion valance state from a +2 state to a higher state, as was previously demonstrated with copper doped Mn spinels.[3,4]

At the same time, the research group headed by Yoshio[14] reported that the coexistence of both oxygen and lithium excess in the spinel matrix is a necessary condition for the 5 V anodic peak observed during SSCV. It was stated also that the intensity of the anodic peak observed at 5 V during SSCV increases as lithium content increases. We assume at this stage that Zn ions are forcing Li ions into 16*d* sites. It is thus suggested that the high anodic peak at 5 V region is related to the extraction of lithium ions from octahedral sites which possess higher lattice energy than the tetrahedral lithium ions.

Conclusions

Zinc doping into $LiMn_2O_4$ materials give rise to the formation of a primitive cubic structure, in contrast to the FCC $LiMn_2O_4$ spinel structure. A partially reversible electrochemical activity at 5 V was recorded with a low doped ($x = 0.25$) Zn substituted $LiZn_xMn_{2-x}O_4$. As expected, almost no electrochemical activity was recorded with the highly doped ($x = 0.5$) Zn substituted analog. On one hand, zinc doping cannot be regarded as the origin of the 5 V electrochemical behavior, and on the other hand, Zn doping is proven to be necessary to facilitate the 5 V behavior.

The full version of the paper will provide detailed structural characteristics of the changes in the $LiMn_2O_4$ on Zn substitution. Zn doping is distinct from analogous doping with Cu, Cr, and other transition elements,[3,9,12] where the original spinel framework was maintained to significant levels of doping. The significant findings reported in this short communication are that the strong tetrahedral site preference of divalent Zn cation is forcing Li cation onto octahedral sites in this material, thus causing electroactivity at 5 V from the displaced Li in the 16*d* sites of the spinel. This application of divalent doping of a nonredox active element, such as Zn in these high-substituted compositions in cubic $LiMn_2O_4$, has not been reported previously. Doping with s^2d^{10} elements such as Zn seems to have unique characteristics, wherein Mn-oxygen framework is influenced, unlike the effect of charge compensation observed with other transition metal dopants (such as Cr, Cu etc.). The effect of such changes in Mn-O coordination may shed some insights into understanding the overall 5 V behavior of undoped Mn-Spinel. The full version of this paper will present in detail the changes in the Mn-oxygen framework due to Zn substitution at high and low potentials (below 3 V). This will include synchrotron based *in situ* XRD, refinement of the structure by Rietvild analysis and XANES as well as electrochemical mapping of more Zn substituted Mn spinel compounds ($0.5 > x > 0$ in $LiZn_xMn_{2-x}O_4$).

Acknowledgments

This work was supported by the Research Foundation of the Technion-Israel Institute of Technology by the Miami Energy Research Fund (grant no. 2003446) and by the Assistant Secretary for Energy Efficiency and Renewable Energy, Office of Transportation Technologies, Electric and Hybrid Propulsion Division, USDOE under contract DE-AC02-98CH10886.

Technion-Israel Institute of Technology assisted in meeting the publication costs of this article.

References

1. T. Ohzuku, M. Kitagawa, and T. Hirai, *J. Electrochem. Soc.*, **137**, 769 (1990).
2. M. M. Thackeray, Y. Shao-Horn, A. J. Kahaian, K. D. Kepler, E. Skinner, J. T. Vaughey, and S. A. Hackney, *Electrochem. Solid-State Lett.*, **1**, 7 (1998).
3. Y. Ein-Eli, W. F. Howard, S. H. Lu, S. Mukerjee, J. McBreen, J. T. Vaughey, and M. M. Thackeray, *J. Electrochem. Soc.*, **145**, 1238 (1998).
4. Y. Ein-Eli and W. F. Howard, *J. Electrochem. Soc.*, **144**, L205 (1997).
5. J. M. Tarascon, W. R. McKinnon, F. Coowar, T. N. Bowmer, G. Amatucci, and D. Guyomard, *J. Electrochem. Soc.*, **141**, 1421 (1994).
6. G. T.-K. Fey, C.-Z. Lu, and T. P. Kumar, *J. Power Sources*, **115**, 332 (2003).
7. T. Ohzuku, S. Takeda, and M. Iwanaga, *J. Power Sources*, **81-82**, 90 (1999).
8. Y.-S. Lee, Y. M. Todorov, T. Konishi, and M. Yoshio, *ITE Lett. Batt., New Technol. Med.*, **1**, 883 (2000).
9. Q. Zhong, A. Banakdarpour, M. Zhang, Y. Gao, and J. R. Dahn, *J. Electrochem. Soc.*, **144**, 205 (1997).
10. A. L. G. L. Salle, A. Verbaere, Y. Piffard, and D. Guyomard, *NATO ASI Ser., Ser. 3*, **85**, 241 (2000).
11. C. Sigala, D. Guyomard, A. Verbaere, Y. Piffard, and M. Tournoux, *Solid State Ionics*, **81**, 167 (1995).
12. S. Mukerjee, X. Q. Yang, X. Sun, S. J. Lee, J. McBreen, and Y. Ein-Eli, *Electrochim. Acta*, **49**, 3373 (2004).
13. J. B. Bates, D. Lubben, N. J. Dudney, and F. X. Hart, *J. Electrochem. Soc.*, **142**, L149 (1995).
14. X. Wang, N. Iltchev, H. Nakamura, H. Noguchi, and M. Yoshio, *Electrochem. Solid-State Lett.*, **6**, A99 (2003).
15. M. M. Thackeray, *J. Electrochem. Soc.*, **144**, L100 (1997).
16. J. H. Kim, C. S. Yoon, S. T. Myung, J. Prakash, and Y. K. Sun, *Electrochem. Solid-State Lett.*, **7**, A216 (2004).
17. Y. Shin and A. Manthiram, *Electrochem. Solid-State Lett.*, **6**, A249 (2003).
18. Y. J. Lee, S.-H. Park, C. Eng, J. B. Parise, and C. P. Grey, *Chem. Mater.*, **14**, 194 (2002).
19. F. A. Cotton, G. Wilkinson, in *Advanced Inorganic Chemistry*, 5th ed., p. 597, John Wiley & Sons, New York (1988).